

# PROTON-ANTIPROTON ANNIHILATION into $\pi^0\pi^0\pi^0$ , $\pi^0\pi^0\eta$ and $\pi^0\eta\eta$ at 900 MeV/c

C. AMSLER

*Physik-Institut der Universität Zürich  
Winterthurerstrasse 190, CH-8057 Zürich*

## Abstract

Crystal Barrel data for proton-antiproton annihilation in flight at 900 MeV/c are presented. The channels  $\bar{p}p \rightarrow \pi^0\pi^0\pi^0$ ,  $\pi^0\pi^0\eta$  and  $\pi^0\eta\eta$  are used to search for isoscalar  $0^{++}$  and  $2^{++}$  mesons in the mass range 1500 – 2000 MeV, which is not accessible with stopping antiprotons. Both  $\pi^0\pi^0\pi^0$  and  $\pi^0\eta\eta$  data sets require an isoscalar  $2^{++}$  resonance decaying into  $\pi^0\pi^0$  and  $\eta\eta$  with mass  $M = (1867 \pm 46)$  MeV and width  $\Gamma = (385 \pm 58)$  MeV. The analysis of  $\pi^0\pi^0\eta$  leads to an isovector  $2^{++}$  state decaying into  $\pi^0\eta$  ( $M = (1698 \pm 44)$  MeV,  $\Gamma = (265 \pm 55)$  MeV). The  $\pi^0\eta\eta$  data show a strong  $f_2'(1525)$  signal, larger than predicted by the OZI rule. The  $\pi^0\pi^0\pi^0$  and  $\pi^0\eta\eta$  data do not show any  $f_0(1710)$ . This adds supportive evidence that this meson is mainly  $s\bar{s}$ .

## 1 Introduction

Scalar ( $0^{++}$ ) mesons overpopulate the mass spectrum below 2 GeV. Table 1 shows a possible SU(3) classification of these states. The low mass scalars are interpreted as scattering resonances [1]. Alternatively, the  $a_0(980)$  and  $f_0(980)$  are often referred to as  $K\bar{K}$  molecules or  $q^2\bar{q}^2$  states [2, 3]. In the literature the narrow  $f_0(1500)$  and  $f_0(1710)$  compete for being the ground state glueball. Recent data in  $\bar{p}p$  annihilation and in central production show that both the  $f_0(1370)$  and  $f_0(1500)$  couple mainly to pions [4, 5] while  $f_0(1710)$  couples mainly to kaons [5]. I will show in this presentation that  $f_0(1710)$  is most likely dominantly  $s\bar{s}$ . This then adds evidence for  $f_0(1500)$  to be mainly gluonic, while  $f_0(1370)$  is the  $u\bar{u} + d\bar{d}$  isoscalar meson [6]. More complicated schemes have been proposed. For a detailed discussion and for a bibliography see refs. [7, 8].

The tensor ( $2^{++}$ ) ground state nonet is well established, but a tentative classification of  $2^{++}$   $q\bar{q}$  excitations, which lie above 1500 MeV, is not possible. This is due to the lack of systematic data in two-body decays like  $\pi\pi$ ,  $K\bar{K}$  and  $\eta\eta$ , very much in contrast to the range below 1500 MeV, which was extensively studied at LEAR. The Particle Data Group [9] lists 9 isoscalar mesons above the  $f_2'(1525)$ , while 6 are expected between roughly 1600 and 2400 MeV ( $2^3P_2$ ,  $3^3P_2$  and  $1^3F_2$  nonets).

$I = 1$	$I = 0$	$I = 0$	$I = 1/2$	Nature
$a_0(980)$	$f_0(400 - 1200)$ (or $\sigma$ )	$f_0(980)$	$\kappa(900)$	Scattering resonances
$a_0(1450)$	$f_0(1370)$ $f_0(1500)$	$f_0(1710)$	$K_0^*(1430)$	$1^3P_0(q\bar{q})$
?	$f_0(2020)$	$f_0(2200)$	$K_0^*(1950)$	$2^3P_0(q\bar{q})$

Table 1: Tentative SU(3) assignment of scalar mesons. The first isoscalar (second column) couples strongly to pions, the second (third column) strongly to kaons. The “pionic” states are very broad, except  $f_0(1500)$ , which is supernumerary.

The  $2^{++}$  glueball is predicted in the upper part of this range [10]. In this talk I will show the evidence for three tensor mesons perhaps building up the  $2^3P_2$  nonet.

## 2 Annihilation at 900 MeV/c

This paper presents the analyses of proton-antiproton annihilation in flight at 900 MeV/c, corresponding to a c.m.s. energy of 2050 MeV, into the three final states  $\pi^0\pi^0\pi^0$ ,  $\pi^0\pi^0\eta$  and  $\pi^0\eta\eta$ , leading to six detected photons [11].

The analysis is based on 17.9 million events which were taken with the all-neutral trigger during the last data taking run of Crystal Barrel at LEAR in 1996. The offline analysis required complete reconstructed events with exactly six clusters and no charged tracks. Figure 1 shows a two-dimensional scatterplot of the  $2\gamma$  invariant mass for kinematically fitted  $\pi^0 4\gamma$  events (imposing momentum and energy conservation). Clear signals for  $\pi^0\pi^0\pi^0$ ,  $\pi^0\pi^0\eta$  and  $\pi^0\eta\eta$  are observed.

The three annihilation channels were selected by applying kinematic fits requiring also three pairs of  $2\gamma$  invariant masses to match the  $\pi^0$  or  $\eta$  masses. For measurements in flight the annihilation vertex of neutral events was not observed and had therefore to be determined by the kinematic fit. Due to the small transverse size of the LEAR beam, the annihilation vertex was assumed to lie on the detector axis. The coordinate along the beam direction was then determined by the fit. The center of the target was found to be displaced by 4.5 mm with respect to the detector center (fig. 1). Since this displacement had to be taken into account for the energy calibration of the crystals (from the measured  $\gamma$  angles in  $\pi^0 \rightarrow \gamma\gamma$  decays), an iterative procedure had to be applied to determine the energies of the photons. The data selection presented here is therefore at variance with the one reported in ref. [12] which assumed a vertex at the center of the detector and therefore incorrect  $\gamma$  energies and angles.

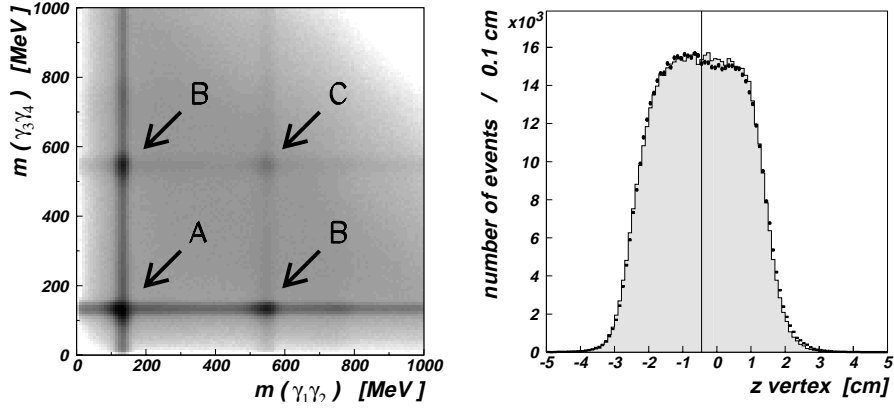


Figure 1: Left: Invariant mass  $m(\gamma_1\gamma_2)$  versus  $m(\gamma_3\gamma_4)$  for kinematically fitted  $\bar{p}p \rightarrow \pi^0\gamma_1\gamma_2\gamma_3\gamma_4$  events (6 entries per event, logarithmic intensity scale). One observes  $\pi^0\pi^0\pi^0$  (A),  $\pi^0\pi^0\eta$  (B) and  $\pi^0\eta\eta$  (C) events. Right: vertex distribution along the beam axis.

The feedthrough from one channel to the other was determined to be less than 0.7%. The reaction  $\bar{p}p \rightarrow \pi^0\omega$  with  $\omega \rightarrow \pi^0\gamma$  (and a missing  $\gamma$ ) was the dominating background channel for  $\pi^0\eta\eta$  and  $\pi^0\pi^0\eta$ . Background contributions of 13% to  $\pi^0\eta\eta$  and 3% to  $\pi^0\pi^0\eta$  were estimated from the data. The background in the  $3\pi^0$  channel was negligible. To avoid an excessive loss of good events, anticuts against  $\omega\pi^0\pi^0$  were not applied. Instead, Monte Carlo simulated events were included in the amplitude analysis described below. We obtained 600,962  $3\pi^0$ , 161,158  $\pi^0\pi^0\eta$  and 18,419  $\pi^0\eta\eta$  events with a detection and reconstruction efficiency of about 27%. The ratio of cross sections of  $\pi^0\pi^0\pi^0$ ,  $\pi^0\pi^0\eta$  and  $\pi^0\eta\eta$  in  $\bar{p}p$  annihilation at 900 MeV/c are  $\pi^0\pi^0\pi^0 : \pi^0\pi^0\eta : \pi^0\eta\eta = 1 : 0.66 \pm 0.02 : 0.17 \pm 0.01$ . These numbers are corrected for reconstruction efficiencies and for the unobserved  $\pi^0$  and  $\eta$  decay modes.

The symmetrised  $\pi^0\pi^0\pi^0$  Dalitz plot is shown in fig. 2 (left). One observes the  $f_2(1270)$ , the  $f_0(1500)$  and/or  $f_2(1565)$ . A faint dip in the 1500 MeV band around 1000 MeV corresponds to the  $f_0(980)$  interfering destructively with the structure at 1500 MeV. Figure 2 (right) shows the Dalitz plot for  $\pi^0\pi^0\eta$ . One observes the  $f_2(1270)$ , the  $f_0(980)$ , the  $f_2(1270)$ , and the  $a_0(980)$ . The symmetrised  $\pi^0\eta\eta$  Dalitz plot and the  $\eta\eta$  mass projections are shown in Figure 3. One observes the  $a_0(980)$ , the  $a_2(1320)$ , the  $f_0(1500)$ , and/or  $f_2'(1525)$ , and a band around 1000 MeV from the  $a_0(980)$ . In the region of the  $f_0(1710)$ , only the interference of the two  $a_0(980)$  bands can be observed and no obvious signal is present (arrow D).

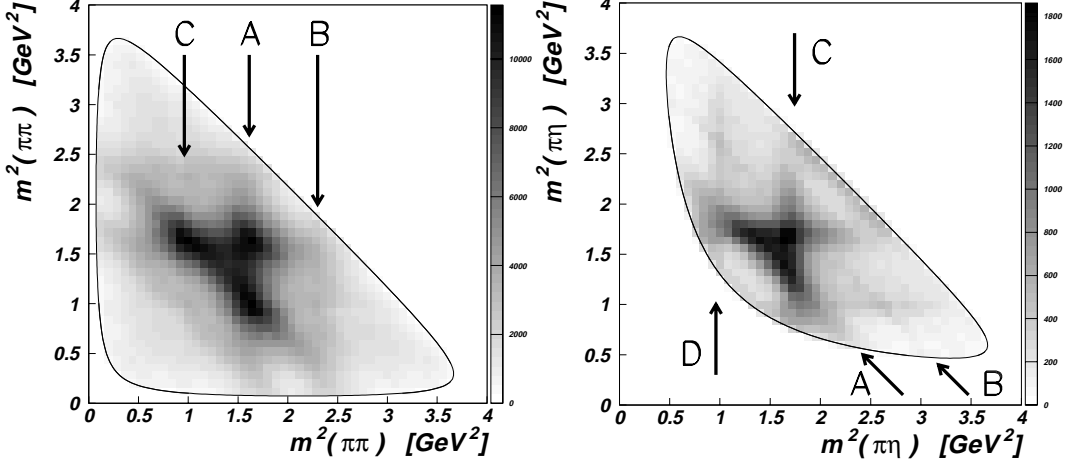


Figure 2: Left: Dalitz plot for  $\bar{p}p \rightarrow \pi^0\pi^0\pi^0$  (six entries per event) with  $f_2(1270)$  (A),  $f_0(1500)$  (B),  $f_0(980)$  (C). Right: Dalitz plot for  $\bar{p}p \rightarrow \pi^0\pi^0\eta$  (two entries per event) with  $f_2(1270)$  (A),  $f_0(980)$  (B),  $a_2(1320)$  (C) and  $a_0(980)$  (D).

### 3 Analysis method

The data sets were analysed in the helicity formalism in terms of the isobar model, in which the  $\bar{p}p$  system is assumed to decay into the three-body final states through a two-body intermediate state made of a resonance and a spectator meson. The transition amplitude for this process, where the  $\bar{p}p$  system has given  $J^{PC}$  and helicity  $M$ , is expressed as

$$A_M^{J^{PC}} = \sum_{\nu,\lambda} H_\nu^{J^{PC}} \cdot f_{\lambda,M}(\Omega, \Omega') \cdot \hat{F}(m), \quad (1)$$

where the sum extends over all possible initial and final state helicities  $\nu$  and  $\lambda$ . The complex constants  $H_\nu^{J^{PC}}$  describe the production process of the  $\bar{p}p$  system. The amplitudes  $f_{\lambda,M}(\Omega, \Omega')$ , where  $\Omega$  and  $\Omega'$  are the production and decay angles, parametrise the angular dependence of the decay [13].  $\hat{F}(m)$  is a dynamical function in the K-matrix formalism which is used to describe resonances in partial waves of given quantum numbers [14]. In the case of a single resonance coupling to one decay channel only,  $\hat{F}(m)$  reduces to a Breit-Wigner amplitude [15]. Since neither beam nor target was polarised, the total transition probability  $w$  for each event is given by the incoherent sum over  $\bar{p}p$  spin-singlet and spin-triplet amplitudes with different helicities  $M$ :

$$w = \left| \sum A_{M=0}^{S=0} \right|^2 + \left| \sum A_{M=-1}^{S=1} \right|^2 + \left| \sum A_{M=0}^{S=1} \right|^2 + \left| \sum A_{M=+1}^{S=1} \right|^2. \quad (2)$$

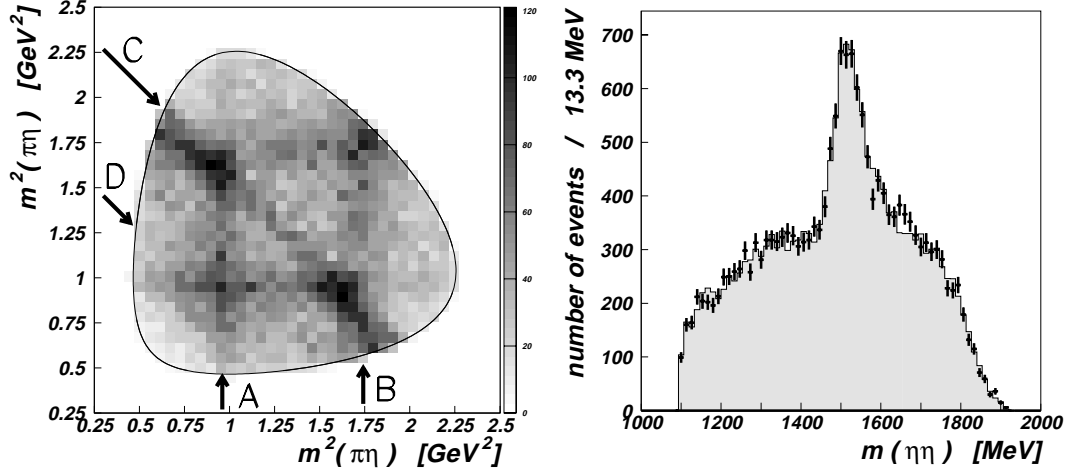


Figure 3: Left: Dalitz plot for  $\bar{p}p \rightarrow \pi^0 \eta \eta$  (two entries per event) with  $a_0(980)$  (A),  $a_2(1320)$  (B),  $f_0(1500)/f'_2(1525)$  (C). Right:  $\eta\eta$  mass projection showing the  $f_0(1500)/f'_2(1525)$ . The long tail is due to the new  $f_2(1870)$ . The histogram is the final fit discussed in the text.

Masses and widths are given by the complex poles of the  $T$ -matrix [14].

While annihilation at rest in liquid hydrogen proceeds mainly from  $S$ -states, more initial states are contributing with increasing energies. The  $J = 4$  contributions to the data sets was found to be less than 5 % and contributions from  $J \geq 4$  were therefore neglected. The following initial partial waves were included in the analysis of the present data:  $^1S_0$ ,  $^3P_1$ ,  $^3P_2 + ^3F_2$ ,  $^1D_2$ , and  $^3F_3$

The  $(\pi\pi)_S$ -wave was parametrised as a  $(3 \times 3)$   $K$ -matrix with four poles corresponding to the  $f_0(400-1200)$ ,  $f_0(980)$ ,  $f_0(1370)$  and  $f_0(1500)$ . The parametrisation was taken from the analysis of the  $\pi^0\pi^0\pi^0$ ,  $\pi^0\pi^0\eta$  and  $\pi^0\eta\eta$  final states at rest [16]. A possible  $f_0(1710)$  was parametrised as a Breit-Wigner amplitude since it is reported to be rather narrow [9]. The  $(\pi\eta)_S$ -wave was parametrised as  $(2 \times 2)$   $K$ -matrix with couplings to  $\pi\eta$  and  $K\bar{K}$  and poles for the  $a_0(980)$  and  $a_0(1450)$  [16]. The  $(3 \times 3)$   $K$ -matrix with four poles from  $\bar{p}p$  annihilation at rest was used for the  $(\eta\eta)_S$ -wave [16]. For the other resonances the masses and widths were taken from the PDG tables [9].

Since there are four independent kinematic variables we performed a maximum likelihood fit. To fit the  $\pi^0\pi^0\pi^0$  and  $\pi^0\pi^0\eta$  data sets the program was ported to the NEC SX-5 supercomputer of the Swiss CSCS facility in Manno. A typical fit took about 10 hours.

## 4 Results

The first description of  $\pi^0\pi^0\pi^0$  included the  $(\pi\pi)_S$ -wave and the  $f_2(1270)$ . The fit was then extended with a second pole in the  $(\pi\pi)_D$ -wave to test for a spin 2 meson. The fit clearly required a high-mass tensor state around 1870 MeV. The best fit was obtained by parametrising the  $(\pi\pi)_D$ -wave as  $K$ -matrix with three poles:  $f_2(1270)$ ,  $f_2(1565)$  and a broad new tensor state with mass  $1877 \pm 30$  MeV and width  $318 \pm 55$  MeV, which we call  $f_2(1870)$ . An  $f_0(1710)$ , parametrised as Breit-Wigner, was also offered to the fit. The contribution was  $(0.8 \pm 0.5) \%$  and the improvement in the likelihood value was not significant. The upper limit for the contribution of the  $f_0(1710)$  to  $\pi^0\pi^0\pi^0$  is 1.5 % at 90 % confidence level (compared to a signal from  $f_0(1500)$  contributing  $(10 \pm 2) \%$ ). The  $\pi\pi$  mass projection is shown in fig. 4.

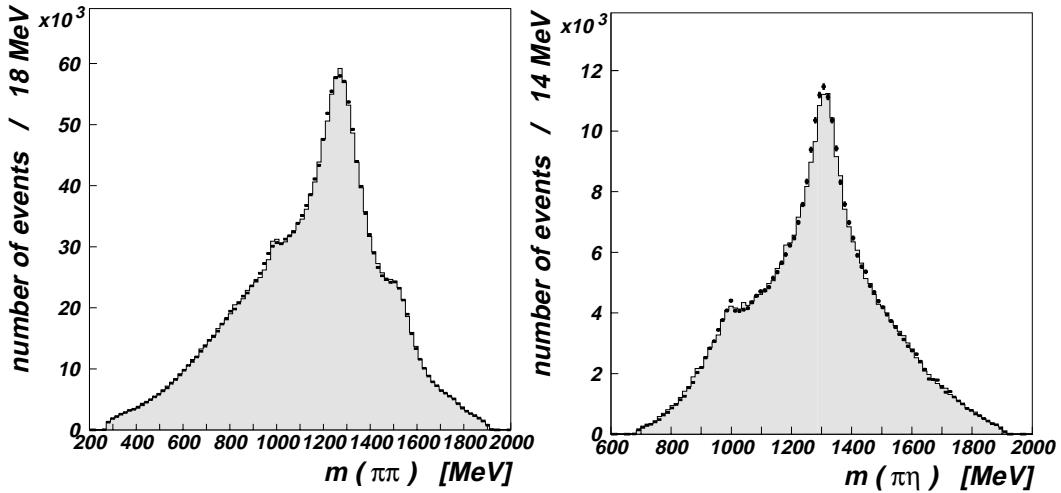


Figure 4: Left:  $\pi^0\pi^0$  mass projection in the  $3\pi^0$  channel. The histogram shows the best fit. The peaks are due to  $f_0(980)$ ,  $f_2(1270)$  and  $f_0(1500)/f_2(1565)$ , and the long tail to the new  $f_2(1870)$ . Right:  $\pi^0\eta$  mass projection in the  $2\pi^0\eta$  channel. The peaks are due to  $a_0(980)$  and  $a_2(1320)$ .

The first description of  $\pi^0\pi^0\eta$  consisted of the  $(\pi\pi)_S$ -wave, the  $f_2(1270)$ , the  $a_0(980)$  and  $a_0(1450)$  in the  $(\pi\eta)_S$ -wave, and the  $a_2(1320)$ . Crystal Barrel reported in  $\pi^0\eta\eta$  at  $1940 \text{ MeV}/c$  an isovector state at  $1660 \text{ MeV}$ , decaying into  $\pi^0\eta$  [17]. Hence this  $a_2(1660)$  was introduced into the  $(1 \times 1)$   $K$ -matrix of the  $(\pi\eta)_D$ -wave as a second pole. The fit improved significantly. The fitted projections together with the data are shown in fig. 4. The  $a_2(1660)$  contributes with

$(7 \pm 2)$  % to the data and for this  $2^{++}$  isovector state we find

$$M = 1698 \pm 44 \text{ MeV}, \Gamma = 265 \pm 55 \text{ MeV}, \quad (3)$$

in excellent agreement with our result in  $\pi^0\eta\eta$  at 1940 MeV/c [17]. The contribution to  $\pi^0\pi^0\eta$  of exotic  $1^{-+}$  resonances like  $\pi_1(1400)$ , decaying into  $\pi^0\eta$ , was found to be completely negligible.

The first description of  $\pi^0\eta\eta$  included in the  $(\pi\eta)_S$ -wave the  $a_0(980)$  and the  $a_0(1450)$ , and the  $a_2(1320)$  in the  $(\pi\eta)_D$ -wave. Significant differences between fit and data were observed for  $\eta\eta$  masses around 1500 – 1550 MeV and 1650 – 1800 MeV. To describe the  $\eta\eta$  peak at 1500 MeV, the tensor resonance  $f_2'(1525)$  was introduced. A good agreement with data could be obtained in the high mass region by adding a high mass tensor state. For this fit the  $(\eta\eta)_D$ -wave was parametrised as a  $(1 \times 1)$   $K$ -matrix with two poles and couplings to  $\eta\eta$  in order to also include the  $f_2'(1525)$ . The resulting  $T$ -matrix poles of the  $(\eta\eta)_D$ -wave were  $m = (1516 \pm 10)$  MeV and  $\Gamma = (74 \pm 11)$  MeV for the  $f_2'(1525)$ , and  $m = (1820 \pm_{10}^{57})$  MeV and  $\Gamma = (358 \pm 42)$  MeV for  $f_2(1870)$ . The parameters of the former agree well with the PDG values [9]. The mass and width of the latter agree with the ones found in the analysis of  $\pi^0\pi^0\pi^0$ .

The  $\eta\eta$  invariant mass projection is shown in fig. 3. The data description is good and there are no significant deviations. The  $f_0(1500)$  contributes with  $(10 \pm 2)$  %, the  $f_2'(1525)$  with  $(15^{+1}_{-3})$  %. As in  $\pi^0\pi^0$ , the inclusion of the  $f_0(1710)$  in the  $\eta\eta$  S-wave was not successful. The  $f_0(1710)$  is not required to describe the  $\pi^0\eta\eta$  data set.

Since the analyses of  $\pi^0\pi^0\pi^0$  and  $\pi^0\eta\eta$  require a high-mass isoscalar tensor state, the data sets were simultaneously fitted with a common description of the resonances, e.g. the  $f_2(1870)$  (for  $\pi^0\pi^0\eta$  this state lies far above the phase space limit).

The fitted Dalitz plots and projections for the two data sets differ only marginally from the ones obtained by the single fits. The  $T$ -matrix pole parameters of the isoscalar  $D$ -wave are listed in table 2. All these parameters are compatible with the values found in the separate analyses. The  $f_2'(1525)$  and  $f_2(1565)$  parameters are compatible with the ones from the PDG tables [9]. We derive an upper limit for the contribution of the  $f_0(1710)$  to  $\pi^0\pi^0\pi^0$  and  $\pi^0\eta\eta$  of 2.1 % and 2.6 %, respectively, at 90 % confidence level, assuming  $m = 1715$  MeV,  $\Gamma = 125$  MeV [9].

	Mass [MeV]	Width [MeV]
$f_2(1270)$	1275	185
$f_2'(1525)$	$1508 \pm 9$	$79 \pm 8$
$f_2(1565)$	$1552 \pm 13$	$113 \pm 23$
$f_2(1870)$	$1867 \pm 46$	$385 \pm 58$

Table 2:  $T$ -matrix pole parameters of the  $(\pi\pi)_D$  and  $(\eta\eta)_D$ -waves of the coupled fit. The  $f_2(1270)$  parameters are fixed.

## 5 Discussion and conclusions

The relative strength of the  $f_0(1500)$  decaying into  $\eta\eta$  and  $\pi^0\pi^0$  in the present analysis,

$$\frac{B(f_0(1500) \rightarrow \eta\eta)}{B(f_0(1500) \rightarrow \pi^0\pi^0)} = 0.24 \pm 0.10, \quad (4)$$

is somewhat smaller but compatible with the value found in the coupled channel analysis at rest,  $0.47 \pm 0.18$  [16].

The partial wave analysis of  $\pi^0\eta\eta$  showed that the  $f_2'(1525)$  is definitely required to describe the data. The quark line rule states that the production of neutral resonances in  $\bar{p}p$  annihilation occurs through the  $u\bar{u} + d\bar{d}$  part of their wave-functions (assuming no valence strange quarks in the nucleon). The ratio of production rates of the two isoscalar members is related to the mixing angle in the corresponding nonet. For the tensor mesons  $f_2(1270)$  and  $f_2'(1525)$  this ratio is

$$\frac{B(\bar{p}p \rightarrow f_2'(1525)\pi^0)}{B(\bar{p}p \rightarrow f_2(1270)\pi^0)} = \frac{\rho_{f_2'}}{\rho_{f_2}} \tan^2(\theta_{2^{++}} - 35.3^\circ), \quad (5)$$

where  $\theta_{2^{++}}$  denotes the mixing angle of the  $2^{++}$  nonet. Using for the phase space factors  $\rho$  the Vandermeulen prescription [18] and  $\theta_{2^{++}} = (25.3 \pm 1.1)^\circ$  from ref. [4], one expects this ratio to be  $0.025 \pm 0.007$ , while we find from the present data  $0.13 \pm 0.05$ . The contribution of the  $f_2'(1525)$  stems mainly from high angular momentum states, in particular  $^1D_2$  and  $^3P_2$ . A large and compatible value of  $R$  was reported by the Obelix Collaboration in  $\bar{p}p$  annihilation at rest in gas [19], where initial  $P$ -wave contributions are large. A similar enhancement is observed in various channels at rest, e.g. in  $\bar{p}p \rightarrow \phi\pi^0$  (for references see [15]).

The fits of  $\pi^0\pi^0\pi^0$  and  $\pi^0\eta\eta$  including an  $f_0(1710)$  were not satisfactory. In the best fit of  $\bar{p}p \rightarrow \pi^0\pi^0\pi^0$  the improvement of the log-likelihood was not significant when the  $f_0(1710)$  was included. When mass and width of the  $f_0(1710)$  were fitted freely in the  $\pi^0\pi^0\pi^0$  and  $\pi^0\eta\eta$  data sets, the resulting object was broad and the other



resonances became unstable. The conclusion was drawn that the  $f_0(1710)$  is not present.

As demonstrated with the  $f_2'(1525)$ , the *observation* of an isoscalar in  $\bar{p}p$  annihilation does not exclude this state to be  $s\bar{s}$ , although the OZI rule forbids the production of pure  $s\bar{s}$  states in  $\bar{p}p$  annihilation. The mechanism for the violation of the OZI rule is not clear and several explanations have been proposed (references can be found in [15]). However, the *absence* of an isoscalar points to a dominant  $s\bar{s}$  component, as there are no obvious mechanisms suppressing a  $u\bar{u}+d\bar{d}$  scalar in  $\bar{p}p$  annihilation. The absence of  $f_0(1710)$  in our data is therefore compatible with an  $s\bar{s}$  assignment. Recent results in central production [5] show that  $f_0(1710)$  prefers to decay into  $K\bar{K}$  rather than into  $\pi\pi$ . This also points to an  $s\bar{s}$  interpretation of the  $f_0(1710)$  and therefore suggests that this meson is the (mainly)  $s\bar{s}$  member of the scalar nonet. It strengthens the interpretation of the  $f_0(1500)$  as a glueball, or as a state with a large gluonic admixture in its wave-function [6].

The best fit to  $\pi^0\pi^0\pi^0$  was obtained including the  $f_2(1565)$  in the  $K$ -matrix parametrisation of the  $(\pi\pi)_D$ -wave. The relative ratio of production in  $\bar{p}p$  annihilation at 900 MeV/ $c$  and decay into  $\pi^0\pi^0$  for the  $f_2(1270)$  and  $f_2(1565)$  is  $0.21 \pm 0.06$ . This is in good agreement with the value found in the analysis at rest,  $0.27 \pm 0.10$  [20]. Hence the  $f_2(1565)$ , which was so far only observed at rest, is confirmed in flight.

The analysis of  $\bar{p}p \rightarrow \pi^0\pi^0\eta$  clearly showed that the  $(\pi\eta)_D$ -wave requires two poles, corresponding to the  $a_2(1320)$  and its radial excitation  $a_2(1660)$ . The L3 collaboration analysing  $\gamma\gamma \rightarrow \pi^+\pi^-\pi^0$  also reported a  $2^{++}$  isovector state in this mass region, decaying into  $\pi^+\pi^-\pi^0$  [21].

The  $\pi^0\pi^0\pi^0$  and  $\pi^0\eta\eta$  data sets require a high-mass tensor  $f_2(1870)$  decaying to  $\pi^0\pi^0$  or  $\eta\eta$ . We do not confirm the narrow  $f_2(1810)$  decaying into  $\pi\pi$  [9]. What is this new state? The relative strength of the  $f_2(1870)$  decaying to  $\eta\eta$  and  $\pi^0\pi^0$  is  $0.27 \pm 0.10$ . This ratio is related to SU(3) mixing angles [6]. One gets two solutions for the mixing angle [11], one being compatible with a pure  $u\bar{u} + d\bar{d}$  state ( $\theta \sim 35.3^\circ$ ), hence a radial excitation of the  $f_2(1270)$ . Then  $f_2(1565)$  and  $f_2(1870)$  are both radial excitations but do not belong to the same nonet. The other solution ( $\theta \sim 15^\circ$ ) leads to a large  $s\bar{s}$  component for  $f_2(1870)$ , in which case  $f_2(1565)$ ,  $a_2(1660)$  and  $f_2(1870)$  could belong to the  $2^3P_2$  nonet. The mass formula then predicts the kaon-like state to lie around 1800 MeV. The ambiguity could be solved by measuring the  $\eta\eta'$  and/or  $K\bar{K}$  decay rates of the  $f_2(1870)$ .

I would like to thank GSI and the organizers for inviting me to this very pleasant and informative workshop.

## References

- [1] J.A. Oller et al., Phys. Rev. D 59 (1999) 074001
- [2] R.L. Jaffe, Phys. Rev. D 15 (1977) 267, 281
- [3] J. Weinstein, N. Isgur, Phys. Rev. D 41 (1990) 2236
- [4] A. Abele et al., Phys. Rev. D 57 (1998) 3860
- [5] D. Barberis et al., Phys. Lett. B 462 (1999) 462
- [6] C. Amsler and F. E. Close, Phys. Rev. D 53 (1996) 295
- [7] C. Amsler, Nucl. Phys. A 663 (2000) 93c
- [8] C. Amsler in Rev. of Particle Physics, Eur. Phys. J. C 15 (2000) 682
- [9] D. E. Groom et al., Rev. of Particle Physics, Eur. Phys. J. C 15 (2000) 1
- [10] C. Michael, Hadron 97 Conf., AIP Conf. Proc. 432 (1998) 657
- [11] M. Heinzelmann, PhD thesis, Universität Zürich, 2000
- [12] A. V. Anisovich et al., Phys. Lett. B 449 (1999) 145, 154
- [13] C. Amsler and J.C. Bizot, Comp. Phys. Commun. 30 (1983) 21
- [14] S. U. Chung et al., Ann. Physik (Leipzig) 4 (1995) 404
- [15] C. Amsler, Rev. Mod. Phys. 70 (1998) 1293
- [16] C. Amsler et al., Phys. Lett. B 355 (1995) 425
- [17] A. Abele et al., Eur. Phys. J. C 8 (1999) 67
- [18] J. Vandermeulen, Z. Phys. C 37 (1988) 563
- [19] A. Alberico et al., Phys. Lett. B 438 (1998) 430
- [20] A. Abele et al., Nucl. Phys. A 609 (1996) 562
- [21] M. Acciarri et al., Phys. Lett. B 413 (1997) 147